

# Quantitative evaluation of the short-lived eddy currents in shield boxes of the novel MRI head coil integrated with PET detectors

Mikio Suga<sup>1,2</sup>, Takayuki Obata<sup>2</sup>, Kodai Shimizu<sup>1</sup>, Fumihiko Nishikido<sup>2</sup>, Atsushi Tachibana<sup>2</sup>, Hideto Kuribayashi<sup>3</sup>, Iwao Nakajima<sup>4</sup>, Yoshihiko Kawabata<sup>4</sup>, and Taiga Yamaya<sup>2</sup>

<sup>1</sup>Chiba University, Chiba, Chiba, Japan, <sup>2</sup>National Institute of Radiological Sciences, Chiba, Chiba, Japan, <sup>3</sup>Siemens Japan K. K., Tokyo, Japan, <sup>4</sup>Takashima Seisakusho Co., Ltd., Tokyo, Japan

## INTRODUCTION

The recent introduction of the use of dual-modality PET/CT imaging has had a profound effect on clinical diagnoses made in radiology, oncology and other areas of nuclear medicine. However, CT images have poor soft-tissue contrast, and PET/CT exposes patients to more radiation than PET itself. PET/MRI can create fusion images with higher contrast than PET/CT. Therefore, the use of PET/MR imaging is more desirable than PET/CT for a hybrid-imaging device. In previous PET/MRI, a PET detector ring was constructed to fit inside a standard MRI. All PET detector components are selected to minimize interference with the MRI. Furthermore, a standard birdcage head coil is mounted on the MR imager bed. Currently, we are developing a new PET/MRI system [1]. This is expected to enable realization of a high-resolution, high-sensitivity and low-cost PET/MRI system by minimizing the size of the PET detector ring through use of a limited number of PET detectors. And, it is compact and easy to add to the conventional MRI system. Scintillators are located in the small ring diameter of the MRI birdcage head coil. To improve spatial resolution, the scintillators were arranged with four-layer DOI (depth of interaction) capability [2]. In this system, PET detectors are closely located at the MR head coil. To reduce electromagnetic interaction between the PET detectors and the MRI coil, the PET detectors are covered with conductive shield boxes. When the magnetic field around the shield box is changed by magnetic field gradient, eddy current is generated in the shield box and a secondary magnetic field appears. The eddy current induces various artifacts in MR images. With short-lived eddy currents, an N half (N/2) artifact appears over the original image. In this study, we quantitatively evaluated the secondary magnetic field induced by short-lived eddy currents in shield boxes and the effect of slits in the shield boxes of the proposed PET/MRI system.

## MATERIALS AND METHODS

Figure 1 shows our prototype MR birdcage head coil integrated with PET shield boxes. The MR head coil can mount eight shield boxes. The shield box is made of acrylic boxes covered with copper foil 35µm thick. In this study, to evaluate the secondary magnetic field induced by the eddy currents from only the shield boxes, the PET detector was not installed in the shield box. A cylindrical phantom filled with a solution of nickel chloride was used as the subject instead. Figure 2 shows the process for imaging the secondary magnetic field due to the eddy currents from the EPI k-space data. The k-space data is separated by even line and odd line [3], and these are transformed to phase images. Using equation 1, the  $\Delta B_0$  map is calculated with phase images.  $\gamma$  is the gyromagnetic ratio,  $\Delta T_s$  is the sampling rate,  $\theta_{even}$  and  $\theta_{odd}$  are phase-image reconstructed even and odd echoes, and  $N_x$  and  $N_y$  are the pixel sizes of read-out and phase-encoding direction. To observe the eddy current reduction effect by making a slit in a shield box, we mounted a shield box without slit on the left side and a shield box with slit on the right side of the head coil. The numbers and positions of slits are shown in the upper part of Figure 3. The width of each slit is 1 mm. Experiments were performed using a Siemens Verio 3T MRI. The imaging protocol was: sequence = spin-echo EPI, repetition time = 7300 ms, echo time = 156 ms, band width = 1002 Hz/pixel, field of view = 500 x 500 mm<sup>2</sup>, image matrix = 192 x 192, slice thickness = 5 mm, number of slices = 9, slice direction = axial. The direction of the EPI read-out gradient that induces eddy currents is sagittal.

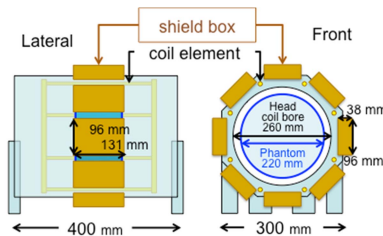


Figure 1. MR birdcage head coil integrated with PET shield boxes

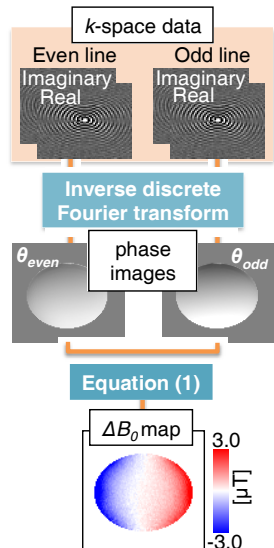


Figure 2. Process of imaging the secondary magnetic field induced by short-lived eddy currents.

$$\Delta B_0(x, y) = \frac{1}{2\gamma N_x \Delta T_s} \left\{ \theta_{even}(x, y) - \theta_{odd}(x, y) - 2\pi \left( \frac{y}{N_y} - \frac{1}{4} \right) \right\} \quad (1)$$

## RESULTS

The magnitude images,  $\Delta B_0$  maps induced by 2 shield boxes, and the average of  $\Delta B_0$  in the left and right ROIs under each condition are shown in Figure 3.  $\Delta B_0$  in the left ROI under all conditions is 1.2 µT.  $\Delta B_0$  in the right ROI under each condition (number of slits = 1, 3, 4 and 6) is 0.9, 0.9, 0.3, 0.2 µT, respectively. We can observe the eddy current reduction effect by making a slit at the yellow line on the shield box.

## CONCLUSION

We developed a prototype MR head coil with shield boxes for PET detectors and quantitatively evaluated the secondary magnetic field due to the short-lived eddy currents in the shield boxes. The results showed that the secondary magnetic field induced by the shield boxes was not negligible for ultra-fast MRI scan (as EPI). So, we must modify the shield boxes to reduce the short-lived eddy currents. For example, we need to insert slits, change the material, etc. The evaluation methods presented here are expected to be useful for the design and optimization of shield boxes.

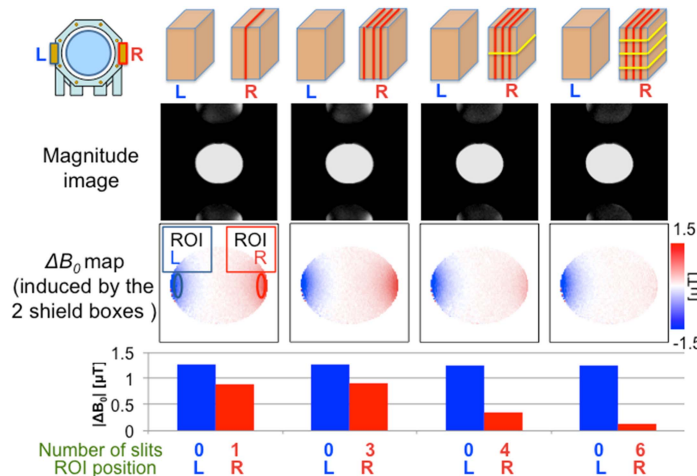


Figure 3. Magnitude images,  $\Delta B_0$  maps induced by the 2 shield boxes, and the average of  $\Delta B_0$  in the left and right ROIs with each number of slits in the shield boxes.

## REFERENCES

- [1] F. Nishikido, et al., Conf. record IEEE NSS/MIC 2012, pp.2750-2752, 2012.
- [2] H. Murayama, et al., IEEE Trans Nucl Sci, 45, pp.1152-7, 1998.
- [3] M. H. Buonocore, et al., MRM, 38:1, pp.89-100, 1997.